Chemical Engineering Journal 327 (2017) 881–888

Contents lists available at ScienceDirect

Chemical Engineering Journal

journal homepage: www.elsevier.com/locate/cej

Phosphorus recovery through biologically induced precipitation by partial nitritation-anammox granular biomass

Sara Johansson, Maël Ruscalleda *, Jesús Colprim

LEQUIA, Institute of the Environment, University of Girona, Campus Montilivi, Carrer Maria Aurèlia Capmany 69, E-17003 Girona, Catalonia, Spain

HIGHLIGHTS

- Partial nitritation-anammox granules induce precipitation of calcium phosphate.
- Granules had an inorganic core of 16 wt% phosphorus.
- Ca/P ratio similar to hydroxyapatite, the presence of which was confirmed by XRD.
- Heavy metals content complied with proposed EU fertilizer limits.
- Potential for a new phosphorus recovery product from urban wastewater.

GRAPHICAL ABSTRACT

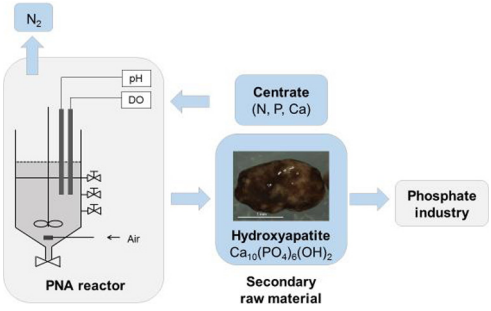

ARTICLE INFO

Article history:
Received 7 February 2017
Received in revised form 22 June 2017
Accepted 23 June 2017
Available online 29 June 2017

Keywords:
Phosphorus recovery
Partial nitritation-anammox
Biologically induced precipitation
Centrate

ABSTRACT

Recovery of phosphorus from waste streams reduces dependence on imported phosphate rock, which is increasingly contaminated with heavy metals and radioactive by-products. This study proves it is possible to recover phosphorus through biologically induced precipitation in granular partial nitritation-anammox sludge. Granules with high inorganic content were harvested from a lab-scale partial nitritation-anammox reactor fed with centrate. Inductively Coupled Plasma (ICP) Optical Emission Spectroscopy showed that the granules had a phosphate content of 36 wt% P_2O_5 and a Ca/P ratio close to that of hydroxyapatite. Crystalline hydroxyapatite was confirmed accordingly by X-ray diffraction. ICP further showed that the metals content complied with fertilizer regulations as well as with requirements from the phosphorus industry. The results are promising as they raise the possibility of recovering phosphorus from urban wastewater without the addition of chemicals.

1. Introduction

The European Union depends on imports of phosphorus for fertilizer production and is facing the declining availability of high-quality phosphate rock [1]. Remaining phosphorus reserves are increasingly contaminated, with cadmium and radioactive by-products the main concern [2]. At the same time, the use of phosphorus is highly inefficient, with large losses occurring throughout the entire food production and consumption system. It is estimated that 20% of the phosphorus mined for fertilizer production ends up in human excreta. This makes wastewater treatment plants (WWTPs) a target for phosphorus recovery [3].

In municipal wastewater treatment plants, the digested sludge liquor (centrate) is a small but concentrated stream, typically contributing 1% of the incoming flow, but 10–30% of the N- and P-load to the plant [4,5]. A separate treatment of this stream is therefore an efficient way to reduce the nutrient load to the water line. The past two decades have seen the implementation of two major processes for nutrient removal and recovery in side-stream conditions: anaerobic ammonium oxidation (anammox) for nitrogen removal and struvite precipitation for phosphorus recovery.

* Corresponding author.
E-mail address: mael@lequia.udg.cat (M. Ruscalleda).

http://dx.doi.org/10.1016/j.cej.2017.06.129
1385-8947/

Partial nitritation coupled with anammox (PNA) reduces the need for organic carbon by 100%, aeration requirements by 60% and sludge production by around 90% compared to conventional nitrification-denitrification [6].

Phosphorus recovery by precipitation of struvite ($MgNH_4PO_4 \cdot 6H_2O$) has been implemented in the full-scale treatment of centrate, for example [7,8]. The precipitation is induced by an increase in pH, through CO_2 stripping or addition of base and addition of a magnesium source. Thus, input is required in terms of aeration energy and chemicals. However, precipitation can also be induced biologically by gradients in ion concentrations and pH created inside or between cells [9]. In Enhanced Biological Phosphorus Removal (EBPR), part of the phosphorus removal is indeed considered to be due to precipitation of calcium phosphate initiated by the elevated phosphate concentrations during anaerobic phosphorus release [10,11]. Similarly, a part of the phosphate removal by aerobic granular sludge has been shown to be due to the formation of calcium phosphate inside the granules [12,13]. The presence of calcium phosphate has also been confirmed in anammox granular sludge and been found to be important for granule mechanical strength [14], as well as functioning as a biomass carrier [15]. Several bacterial strains have also been shown to be able to precipitate struvite [16–18].

Since biomineralization allows for precipitation induced by microorganisms, it offers the possibility of recovering phosphorus without the addition of chemicals. The accumulation of minerals increases the gravity of granules and leads them to settle to the bottom of the reactor where they can be easily harvested [14]. Therefore, phosphate minerals formed through biomineralization have potential as a phosphorus product recovered from wastewater. However, as with any product recovered from wastewater, the presence of harmful substances is a concern and an evaluation of the metals content in calcium phosphate formed by PNA sludge has been lacking.

The current revision of the existing EU fertilizer legislation is proposing to include recovered phosphorus products within the legal framework, as well as introducing limits to heavy metals content in fertilizer [19], both of which will open new opportunities for recovered phosphorus products to enter the market. Although the majority (85%) of mined phosphate rock is used for fertilizer production [3], there is a small but considerable amount used by the elemental phosphorus industry, which has expressed concern about the increasing levels of impurities in phosphate rock [20].

Therefore, in this study, granules with a high inorganic content formed in a lab-scale PNA reactor were evaluated for their possible application as a recovered phosphorus product. The reactor was fed with centrate from a local wastewater treatment plant to ensure real conditions. The structure, chemical composition and type of mineral were studied using microscopy, quantitative elemental analysis and direct spectral analysis. The heavy metals content was analysed and compared to the proposed EU limits for P fertilizer and the requirements from the elemental P industry. In the final sections, some possible biological mechanisms inducing precipitation are suggested.

2. Materials and methods

2.1. PNA reactor operating conditions

A PNA sequencing batch reactor (SBR) (see Fig. 1) with minimum volume of 10 L was started up with 1 L of inoculum from a lab-scale PNA-SBR reactor operated under mainstream conditions. The PNA-SBR reactor was fed with centrate and the temperature was kept at 25 °C using a water jacket. pH and dissolved oxygen (DO) were monitored using probes (Orbipac CPF81 and Oxymax

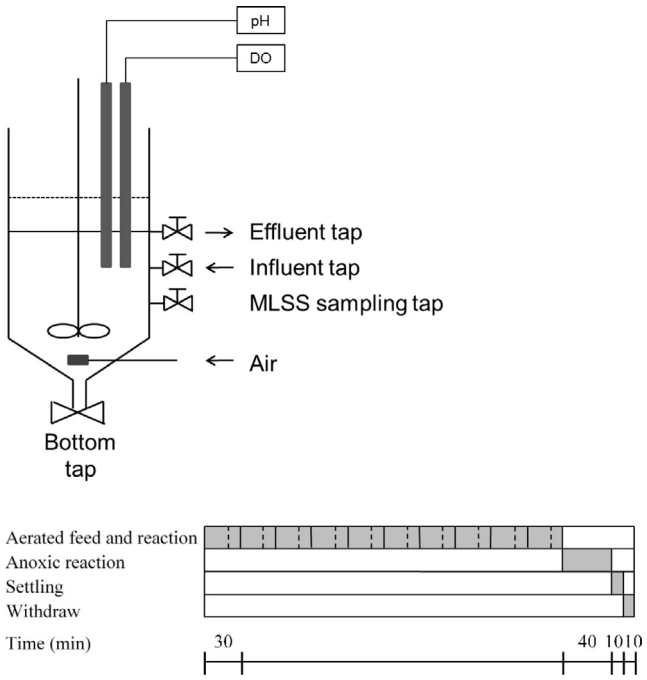

Fig. 1. Reactor layout and cycle configuration.

W COS41 respectively, Endress + Hauser) connected to an online monitoring system (Liquisys M, Endress + Hauser). A 6-h batch cycle was configured as follows: 10 repeated sequences of aerated feed and reaction (30 min each), followed by anoxic reaction (40 min), settling (10 min) and drawing (10 min). The nitrogen load was increased by lengthening the feed and simultaneously decreasing the aerated reaction phase while maintaining the total length of time at 30 min.

2.2. Influent wastewater (centrate)

Centrate was collected every three weeks from WWTP Terri (Cornellà de Terri, Catalonia, Spain), which treats 10,000 m^3 of urban and industrial wastewater per day (design load 186,560 p. e.). At the WWTP, primary and secondary sludge is sent to a mesophilic digester (37 °C) with a residence time of approximately 40 days. Phosphorus is removed chemically using iron chloride, which is dosed prior to the entrance of the secondary settler. After collection, the centrate was kept in a cold storage tank at 4 °C. The centrate had a pH of 8.1 ± 0.2, an ammonium concentration of 966 ± 130 mg N L^{-1}, a P—PO_4 concentration of 57 ± 27 mg P L^{-1}, a calcium concentration of 79 ± 33 mg Ca L^{-1} and an alkalinity concentration of 4401 ± 479 mg $CaCO_3$ L^{-1}. A more detailed description of the composition of the centrate is presented in Section 3.6.

2.3. Analytical characterization of the liquid and solid phases

Effluent was sampled twice a week, while the influent was sampled on the day of collection and then once a week from the cold storage tank. MLSS samples were taken once a week in the beginning of the aerated feed and reaction phase. Analysis of N—NH_4^+, total suspended solids (TSS), volatile suspended solids (VSS) and alkalinity were performed according to Standard Methods [21]. Concentrations of N—NO_2^-, N—NO_3^-, P—PO_4^{3-}, Mg^{2+} and Ca^{2+} were analysed using ion chromatography (Dionex IC5000) after being filtered with 0.2 μm filters. The morphology of the granules was observed with a stereomicroscope (ZEISS Stereo Discovery V12). MLSS samples for X-ray diffraction (XRD) were filtered and then air-dried over night before analysis. The XRD analysis was per-

formed on a Bruker D8 Advance, with Bragg-Brentano Theta-2Theta geometry, reflection mode with Cu Kalpha radiation from an X-ray tube, operated at 40Kv 40mA.

Samples for SEM-EDX (Scaning Electron Microscopy with Energy Dispersive X-ray analysis) were rinsed with milliQ water before analysis. A couple of the granules were cracked open before SEM-EDX analysis in order to study the inside. Another group of granules were cut using a cryo-microtome (PowerTome X, RMC Products) to prepare the samples for elemental mapping. The EDX analysis was performed with a Bruker X-Flash detector 5010, with a detection limit of 129 eV, coupled to an SEM (ZEISS DSM960A).

Heavy metals were analysed using Inductively Coupled Plasma-Mass Spectroscopy (ICP-MS) (Agilent 7500c). Calcium (Ca), phosphorus (P), magnesium (Mg), potassium (K) and iron (Fe) were analysed using Inductively Coupled Plasma-Optical Emission Spectrometry (ICP-OES) (Agilent 5100). The sample for ICP analysis was taken from the bottom of the reactor and rinsed with milliQ water. Subsequently, it was dried at 105 °C overnight. The sample was digested with a mix of nitric and hydrochloric acid in duplicate using an Etos Sel microwave from Milestone. The samples were digested in two steps: ramping up to 180 °C over 10 min and then digested for 20 min at 180 °C.

2.4. Saturation index calculations

The saturation index (SI) was calculated using the software Visual MINTEQ (version 3.0). The degree of saturation, Ω, and the saturation index, SI, with respect to the mineral phases, were defined as:

$$\Omega = \frac{IAP}{K_{sp}} \quad (1)$$

$$SI = \log \Omega = \log IAP - \log K_{sp} \quad (2)$$

where IAP is the ion activity product and K_{sp} is the solubility product of the precipitated mineral. The solution is considered to be oversaturated when the SI is above zero, at saturation when zero and undersaturated when less than zero. The mineral phases considered were hydroxyapatite, calcite and struvite.

3. Results and discussion

3.1. Reactor performance

The reactor was started up with an initial biomass concentration of 0.7 g VSS L^{-1}, which gradually increased as the nitrogen loading rate (NLR) was increased. Because of the low initial VSS concentration, no sludge was wasted during the 200 days that the reactor was in operation for this study. Mean values of the bulk liquid pH, VSS, VSS/TSS ratio, nitrogen loading rate, as well as the nitrogen removal and the molar ratio of NO_3^- produced over NH_4^+ consumed are all shown in Table 1.

The bulk liquid pH was not regulated, and thus the pH was a result of the nitrifying activity of aerobic ammonium oxidizing bacteria (AOB), which has an acidifying effect (Eq. (3)).

$$NH_4^+ + 1.5O_2 \rightarrow NO_2^- + H_2O + 2H^+ \quad (3)$$

An initial increase in the $NO_{3\,prod}^-/NH_{4\,cons}^+$ ratio was noted, indicating growth of nitrite oxidizing bacteria (NOB), but after 50 days of operation, a stable microbial community of aerobic ammonium oxidizing bacteria and anammox with suppressed NOB growth was obtained, as the $NO_{3\,prod}^-/NH_{4\,cons}^+$ ratio was close to the stoichiometric of 0.11. The nitrogen load was gradually increased to 0.308 g N—NH_4^+ L^{-1} d^{-1} and nitrogen removal reached 80%, with specific nitrogen removal of 0.180 g N—NH_4^+ (g VSS)$^{-1}$ d^{-1}.

The feed was stored in a cold storage tank that was initially equipped with a mixer. However, an increase in pH and subsequent precipitation was noted in the tank during storage of the feed, and the mixer was disabled on operational day 80. Subsequently, less precipitation was observed in the storage tank, with a resulting increase of free ions in the feed. After 100 days of operation, a drop in the organic fraction of the MLSS was noted, with a decrease in the VSS/TSS ratio from 92–94% to 65%. The increase in the inorganic fraction of the biomass was therefore assumed to have been initiated by the increased concentration of ions in the feed to the reactor following the disabling of the mixer in the storage tank.

3.2. Granule structure and distribution in reactor

The granules in the MLSS had the typical orange-red colour of anammox biomass. However, after the drop in the VSS/TSS ratio was noted, granules with a dark and hard core were observed. Fig. 2a shows a sample from the MLSS (sampled on operational day 199) observed under the stereomicroscope and the mineral core can be seen embedded in the biomass, indicating that the mineralization was biologically induced. This theory is further strengthened by the fact that no precipitation was noted in the bulk liquid nor any scaling on the walls.

Over time, dark-brown granules with a high inorganic content (>70%) accumulated at the bottom of the reactor. Although the reactor was being mixed, the density of these mineralized granules was too high to keep them in suspension by mixing. The MLSS was therefore separated by gravity, with increasing solids concentration and inorganic content towards the bottom (Table 2). The stratification could also be seen visually, with reddish coloured granules in the MLSS and dark-brown granules at the bottom of the reactor (Fig. 2b). Fig. 2c shows a granule sampled from the bottom of the reactor, with almost no biomass attached, and in Fig. 2d the mineral core remaining after incineration at 550 °C can be seen.

An SEM image from the interior of a granule (Fig. 3) shows a porous beehive-like structure similar to the one observed by Mañas et al. [13] in aerobic granules. This is suggested to be due to precipitate formation around cells. *Epicellular* mineralization, that is, the formation of minerals along the surface of the cell wall, is a typical feature of biologically induced mineralization, as the cell wall is the site of metabolic fluxes of ions in and out of the cell [9].

3.3. Elemental composition and distribution in PNA granules (ICP-OES and SEM-EDX)

Table 3 presents the composition of the granules as measured by ICP-OES. The main elements were calcium (33.5 ± 1.9 wt%) and phosphorus (15.8 ± 0.99 wt%), with some traces of magnesium

Table 1
Mean operational parameters during 200 days of start-up and operation.

Time period (days)	Reactor pH	VSS (g L^{-1})	VSS/TSS (%)	NLR (g N—NH_4 L^{-1}, d^{-1})	N-removal (%)	$NO_{3\,prod}^-/NH_{4\,cons}^+$ (mol mol^{-1})
0–50	7.73	0.79	92	0.085	60	0.19
50–100	7.50	0.90	94	0.148	61	0.12
100–150	7.41	1.07	65	0.214	74	0.09
150–200	7.22	1.45	62	0.308	66	0.10

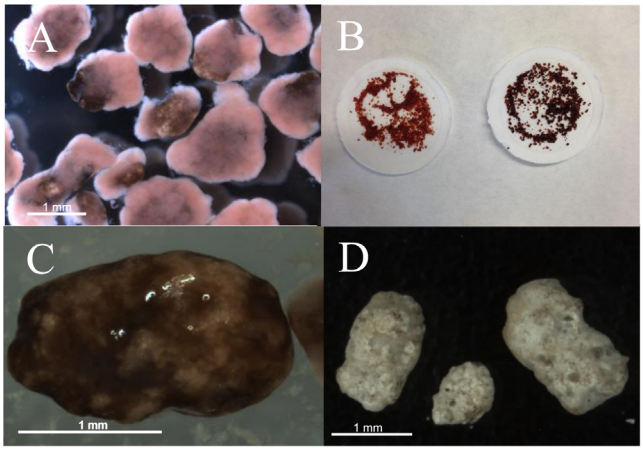

Fig. 2. Granules from the MLSS (a), granules from the MLSS (left) and bottom of reactor (right) (b), granule from the bottom of the reactor (c), inorganic core after incineration at 550 °C (d).

Table 2
Suspended solids and inorganic fraction from different sample taps.

Sample port	TSS (g/L)	Inorganic fraction (% of TSS)
Effluent tap (top)	1.5 ± 0.05	6.4
Influent tap (middle)	1.9 ± 0.00	10
MLSS sampling tap (lower)	2.2 ± 0.03	15
Bottom tap (bottom)	22 ± 5.1	71

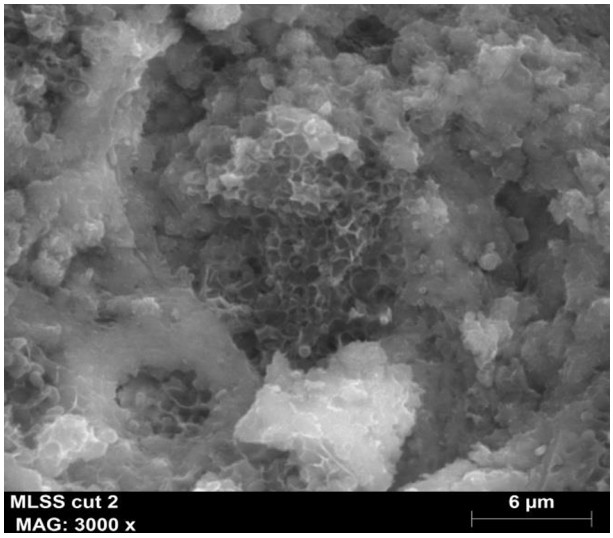

Fig. 3. SEM picture showing the inner part of a granule.

(<1 wt%) and potassium (<1 wt%). The molar ratio of calcium over phosphorus was 1.64, which is close to the theoretical ratio of 1.67 for hydroxyapatite ($Ca_5(PO_4)_3(OH)$). The low amount of magnesium detected excludes the presence of struvite in any major quantities. It should be noted that the phosphorus content is similar to that of phosphate rock, which typically contains 13–17.5 wt % of P [22].

A number of calcium phosphates may form, depending on the pH and solution composition [23], but they are likely to transform into the thermodynamically most stable phase, which at standard conditions is hydroxyapatite. Precursor phases to hydroxyapatite include dicalcium phosphate dehydrate (brushite) (DCPD), octacalcium phosphate (OCP), tricalcium phosphate (TCP) and amorphous

Table 3
Quantitative elemental composition of granules (ICP-OES).

Element	Composition (wt%)
Ca	33.5 ± 1.94
P	15.8 ± 0.99
Mg	0.24 ± 0.00
K	0.12 ± 0.004

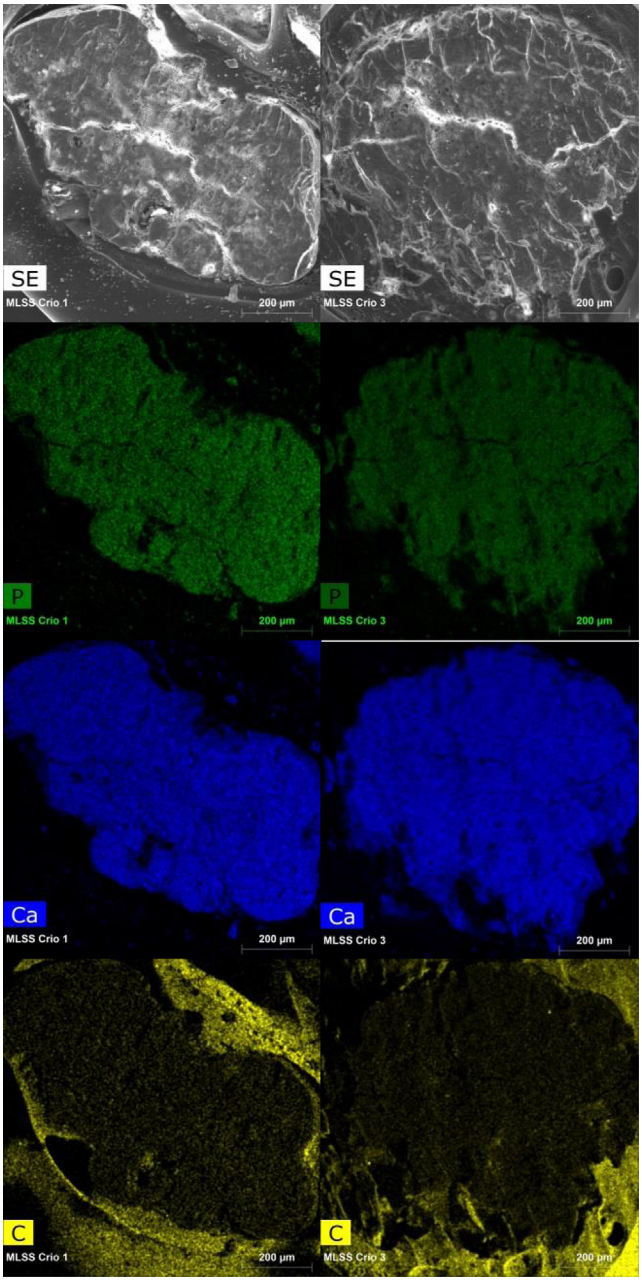

Fig. 4. SEM images of two cryosected granules and elemental mapping using EDX of P, Ca and C.

calcium phosphate (ACP) [23,24]. They all have lower Ca/P ratios compared to hydroxyapatite: ACP 1.5, DCPD 1.0, TCP 1.5 and OCP 1.33, respectively. The presence of hydroxyapatite precursor phases may explain why the Ca/P ratio of the granules is slightly lower than that for hydroxyapatite.

Fig. 4 shows the intersection of two cryosected granules and the elemental mapping of the elements of phosphorus (P), calcium (Ca)

and carbon (C). The elemental mapping reveals a homogenous distribution of phosphorus and calcium over the intersection surface, while carbon was sparsely detected in the centre of the granules but was found on the exterior of the granules. The carbon detected can be associated with biomass and is also present in the coating medium used to prepare the samples for the SEM-EDX.

Apatites (with the general formula $Ca_{10}(PO_4)_6X_2$, X = OH^-, F^-, Cl^-) have a natural affinity for metals [20]. Therefore, it is not unlikely that some metals would be incorporated into the crystal matrix. However, the presence of iron and aluminium was less than 1%, as detected by EDX. The presence of iron and heavy metals will be further discussed in Section 3.5.

3.4. Identification of mineral species in PNA granules by XRD

Fig. 5 shows the XRD diffractogram of a dried and ground sample from the MLSS. It suggests the presence of four types of crystalline calcium phosphates: hydroxyapatite ($Ca_5(PO_4)_3(OH)$), apatite ($(Ca_4Na_{0.01}Mg_{0.02})(Ca_6Na_{0.13}Mg_{0.03})(PO_4)_6$), chloroapatite ($Ca_5(PO_4)_3Cl$) and calcium sulphide phosphate ($Ca_{10}(PO_4)_3S$). A second XRD analysis of dried and ground granules from the bottom of the reactor (data not shown) showed a similar pattern, with the presence of crystalline hydroxyapatite and apatite, and two other crystalline calcium phosphates: oxyapatite ($Ca_{10}(PO_4)_6O$) and fluorapatite ($Ca_5(PO_4)_3F$). It should be noted that the granules sampled from the bottom of the reactor were dried at 105 °C, while the MLSS sample was dried at room temperature. It is possible that the higher temperature caused the dehydration of hydroxyapatite to oxyapatite.

Na and Mg were only detected in minor amounts (<1%) by both EDX and ICP, and S was not detected by any of the methods. Therefore, the presence of calcium phosphates containing these minerals can only be minor and therefore disregarded. Chloride and fluoride are not measured by any of the methods used in this study, so their presence cannot be ruled out. Both chloro- and fluoroapatite are also common members of the apatite family and are naturally found in phosphate rock. However, as they were not coherently detected by XRD, hydroxyapatite is considered to be the main mineral.

The XRD only detects crystalline structures but the background noise suggests the presence of amorphous compounds. The hydroxyapatite precursors are more water soluble, indicating a lower degree of crystallinity compared to hydroxyapatite. Following the results of the ICP analysis, the Ca/P ratio of the granules (1.64) is close to but slightly lower than the theoretical ratio of hydroxyapatite (1.67). The presence of ACP or other amorphous precursor phases may explain the slightly lower Ca/P ratio but also contribute to the background noise detected by XRD.

3.5. Purity of the product (ICP-MS and ICP-OES)

Table 4 shows the content of phosphate (expressed as P_2O_5) and metals in the granules from this study, calcium phosphate pellets recovered through chemical precipitation from wastewater, and average values of phosphate rock reserves and P fertilizer used in Europe. The limits of heavy metals content proposed to be included in the EU Fertilizer Regulation, as well as the requirements of the elemental phosphorus industry, are listed with the phosphorus products in Table 4 for comparison.

The granules recovered from the PNA reactor had a higher phosphate content and comparable or lower content of metals compared to calcium phosphate pellets recovered through chemical precipitation from wastewater and average P fertilizers used in Europe.

The amounts of heavy metals detected in the granules were well within the proposed limits for P fertilizer. The only exception was chromium, where compliance with the proposed EU limits could not be evaluated. This was due to the fact that the EU limits only regulate Cr VI, which is the highly toxic and carcinogenic oxidation state. The ICP analysis done in this study reports chromium as the total amount without specifying the oxidation state. Therefore, the amount of the chromium present in the granule that is found in the form of Cr VI needs to be further examined.

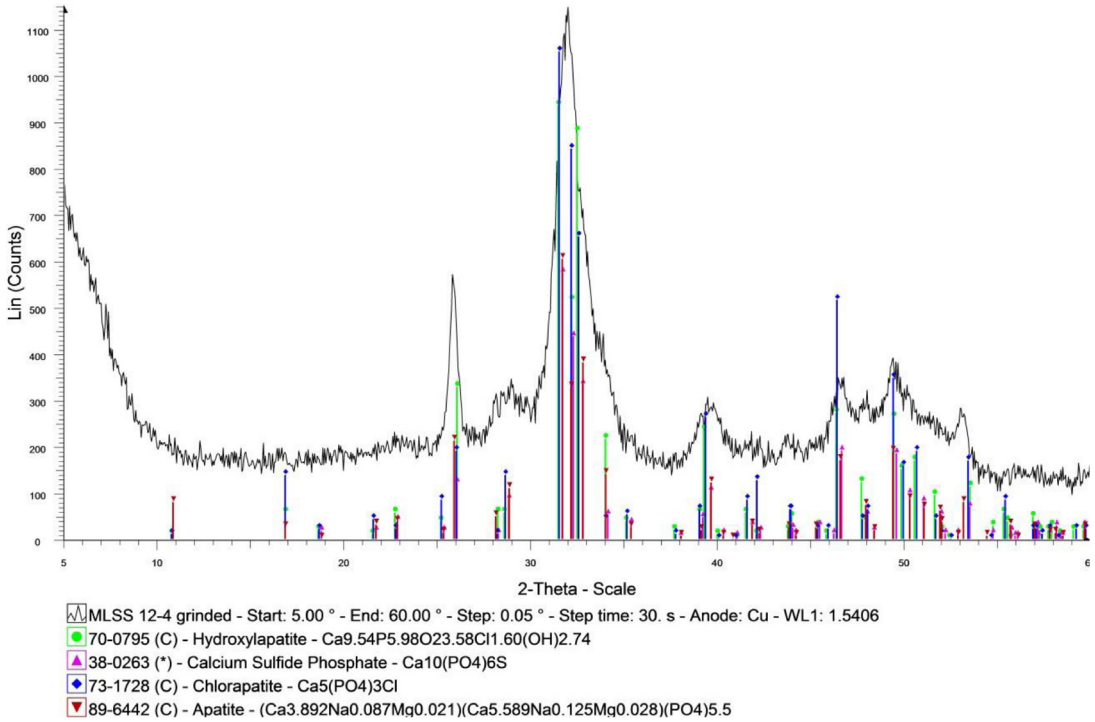

Fig. 5. XRD diffractogram for dried granules from the MLSS.

Table 4
Phosphate and metals content of phosphate products compared to the proposed EU limits for P fertilizer and requirements from the P industry.

Parameter	Unit	Granules[a]	Crystalactor pellet[b]	P fertilizer[c]	Phosphate rock[d]	Requirements P industry[e]	Proposed EU limits[f]
P_2O_5	wt%	36	26	19	36	≥25	≥5
Cd	mg (kg P_2O_5)$^{-1}$	0.041	7.7	38	69	–	20-60[i]
As	mg (kg DW)$^{-1}$	4.7	2	7.6	11	–	60
Cr	mg (kg DW)$^{-1}$	37	8	90	188	–	2[ii]
Cu	mg (kg DW)$^{-1}$	10	–	–	–	500	–
Fe	mg (kg DW)$^{-1}$	878	1260	–	–	10 000	–
Hg	mg (kg DW)$^{-1}$	0.21	–	–	0.05	–	2
Ni	mg (kg DW)$^{-1}$	0.85	8	15	29	–	120
Pb	mg (kg DW)$^{-1}$	0.29	–	2.9	10	–	150
Zn	mg (kg DW)$^{-1}$	25	310	166	–	1000	–

– not determined.
[a] This study (ICP-OES and ICP-MS).
[b] Driver et al. [20].
[c] Mortvedt [25].
[d] Nziguheba and Smolders [26].
[e] Schipper et al. [22].
[f] [27].
[i] 60 mg/kg P_2O_5 at the date of application of the regulation, 40 mg/kg P_2O_5 3 years after application and 20 mg/kg P_2O_5 12 years after application.
[ii] Cr VI.

The phosphorus industry is mainly concerned about a sufficiently high phosphate concentration and, in relation to metals, limited amounts of copper, zinc and iron. The recovered granules passed all of these requirements. Furthermore, phosphate products recovered in the form of calcium phosphate are welcomed by the industry, as the presence of magnesium and ammonium interfere with the process, which has hindered struvite as a secondary phosphate rock candidate [20].

The organic content of the granules sequestered from the bottom of the reactor was less than 30 wt%, but the organic fraction might still have to be removed before the product can be accepted by the industry. Finally, it is of interest to note the metals content in phosphate rock, where the levels of cadmium are especially of concern.

3.6. Inorganic core of hydroxyapatite in PNA granules (SI index calculations)

The mean values of the centrate used during the operation of the reactor are shown in Table 5, alongside the calculated saturation indexes for hydroxyapatite, calcite and struvite. Hydroxyapatite clearly had the highest saturation index, meaning it is thermodynamically the most stable phase under the conditions defined. This corresponds well with the results of the ICP and XRD analyses, which both pointed to hydroxyapatite being the main constituent of the mineral core of the granules.

Calcite and struvite had much lower saturation indexes and, accordingly, neither of these compounds were detected by spectral analysis performed on the granules. The SI calculations were performed on the centrate and, as the PNA process consumes carbonate as well as ammonium, the saturation index for struvite and calcite is expected to be even lower inside the granules.

However, in addition to thermodynamics, kinetics also influence the formation and growth of crystals. Ostwald's rule for multi-phase precipitation of sparingly soluble inorganic salts states that it is not generally the most stable but rather the most soluble phase that crystallizes first. Subsequently, thermodynamic driving forces act to transform the salts into more stable phases [28].

In the case of the formation of crystalline hydroxyapatite, the precursor phases are more water soluble and form first, but the retention of particles provided by the granules then allow for transformation into the stable form of hydroxyapatite that, once formed, has poor water solubility. Thus, the granules allow for the growth and accumulation of an inorganic core of crystalline hydroxyapatite.

Table 5
Centrate composition and SI of hydroxyapatite, calcite and struvite.

Parameter	Unit	Centrate
T	°C	25
pH		8.1 ± 0.2
Alkalinity	(mg $CaCO_3$) L^{-1}	4401 ± 479
N—NH_4^+	mg L^{-1}	966 ± 130
P—PO_4^{3-}	mg L^{-1}	57 ± 27
Ca^{2+}	mg L^{-1}	79 ± 33
Mg^{2+}	mg L^{-1}	14 ± 8
K^+	mg L^{-1}	279 ± 40
Na^+	mg L^{-1}	345 ± 47
Cl^-	mg L^{-1}	507 ± 77
S—SO_4^{2-}	mg L^{-1}	23 ± 8
N—NO_3^-	mg L^{-1}	0.38 ± 0.32
Mineral		SI
Hydroxyapatite		12.9
Calcite		1.66
Struvite		0.56

The findings are in line with other studies on biomineralization in different types of granular sludge, which have also confirmed hydroxyapatite as the prevalent mineral. Mañas et al. [13] confirmed that biologically induced precipitation of hydroxyapatite accounted for 45% of overall P removal in aerobic granules, while Tervahauta et al. [29] demonstrated that hydroxyapatite was present in the inorganic core of anaerobic granules treating black water.

3.7. Biologically induced precipitation of calcium phosphates in PNA granules

In this study, no precipitation or scaling was noted in the bulk liquid or on the walls of the reactor, but only in association with the granular sludge, indicating that the mineralization was biologically induced. The same was reported in a full-scale anammox reactor where apatite was observed [14], indicating that biomineralization is not an uncommon phenomena.

The typical operational pH of a PNA reactor is close to neutral [6], which is lower than for phosphate crystallizers (pH typically > 8) [30]. In this study, the 50-day mean value ranged between 7.2 and 7.7 (see Table 1). However, the physical and biochemical properties of granular PNA sludge makes it act as a biological crystallizer. In PNA granular sludge, the anammox

biomass grows in the inner anoxic zone covered by a layer of aerobic ammonium oxidizing bacteria [31,32]. The granules thus provide stratification in terms of microflora, dissolved oxygen and substrate throughout the biofilm [31,32]. Anammox bacteria anaerobically oxidizes ammonia to nitrogen gas with nitrite as the electron acceptor (see Eq. (4)) [33]. The reduction of carbonate consumes protons, with a subsequent increase in pH. The decrease in carbonate simultaneously decreases the alkalinity, which further facilitates changes in pH. Elevated internal pH has accordingly been measured inside PNA granules [34].

$$NH_4^+ + 1.32NO_2^- + 0.066HCO_3^- + 0.13H^+ \rightarrow 1.02N_2 + 0.26NO_3^- + 2.03H_2O + 0.066CH_2O_{0.5}N_{0.15} \quad (4)$$

Although formation of calcium phosphate minerals in anammox and PNA sludge has been confirmed, the exact microbiological mechanisms are still unknown. It is, for example, not known if the precipitation is linked to a specific strain, or if it is a mere side effect of microbial activity. As pH is one main driver of precipitation, it can be assumed that bulk liquid pH, as well as the anammox activity, could be important factors. The granule size could also have an impact due to mass transfer resistance, and granule size has been shown to impact the inorganic content in aerobic granules [35]. To elucidate the microbiology behind the biomineralization of PNA sludge would be an interesting topic for further research.

3.8. Recovery and utilization of biologically precipitated calcium phosphate

Anammox are slow-growing organisms and PNA sludge is in demand for inoculation of new installations. Therefore, there is a potential conflict between granules for inoculation and harvest of a phosphorus product. However, the experience from both this study and a full-scale anammox installation [14] show that there is stratification inside the reactor, where granules with a high inorganic content settle at the bottom and the granules in the mixed liquor have a higher biomass content. Since the inorganic core is biologically inactive, harvest of these granules should not conflict with demand for sludge for inoculation purposes.

Harvested granules could either be incorporated as a secondary raw material into the current infrastructure where phosphate rock is processed into fertilizer or elemental phosphorus, or spread directly onto fields, as is done with sewage sludge. If used as a secondary raw material in the phosphorus industry, the organic fraction would have to be removed, but because the biomass is attached externally, it should be easier to remove compared to impurities that are incorporated into the mineral, such as the heavy metals present in raw phosphate rock or the magnesium in struvite.

If the harvested product is to be used directly as a fertilizer, it might not be a disadvantage should some biomass remain, as this adds organic material to the soil. The P content of the granules (158 g/kg DW) is higher than that of sewage sludge (typical P content around 30 g/kg DW [36]) and thus the granules represents a concentrated source of P which facilitates handling.

4. Conclusions

Biologically induced precipitation of calcium phosphate was confirmed in PNA granular sludge. Granules with a high inorganic content settled due to gravity, which allowed for easy recovery. Harvested granules showed a high phosphate content (16 wt%), with a Ca/P ratio close to that of hydroxyapatite, the presence of which was confirmed by XRD, although probably coexisting with amorphous calcium phosphates. The metals content complied with proposed EU limits for phosphorus fertilizer as well as with requirements from the phosphorus industry. The calcium phosphate formed without the addition of chemicals and is proposed as a novel phosphorus recovery product from wastewater.

Acknowledgments

The work was financially supported by the European Union's Horizon 2020 research and innovation program under the Marie Sklodowska-Curie grant agreement No 642904.

The authors would like to thank Sunsi Ferrer Matas and the operators of WWTP Terri for their help with the collection of centrate.

References

[1] Science Communication Unit University of the West of England, Science for Environment Policy In- depth Report: Sustainable Phosphorus Use. Report produced for the European Commission DG Environment, 2013.
[2] M. DeRidder, S. de Jong, J. Polchar, S. Lingemann, Risks and Opportunities in the Global Phosphate Rock Market, 2012. doi: Report No 17/12/12, ISBN/EAN: 978-94-91040-69-6.
[3] D. Cordell, J.O. Drangert, S. White, The story of phosphorus: Global food security and food for thought, Global Environ. Change 19 (2009) 292–305, http://dx.doi.org/10.1016/j.gloenvcha.2008.10.009.
[4] M.C.M. van Loosdrecht, S. Salem, Biological treatment of sludge digester liquids, Water Sci. Technol. 53 (2006) 11–20, http://dx.doi.org/10.2166/wst.2006.401.
[5] A. Marchi, S. Geerts, M. Weemaes, S. Wim, V. Christine, Full-scale phosphorus recovery from digested waste water sludge in Belgium – part I: technical achievements and challenges, Water Sci. Technol. 71 (2015) 487, http://dx.doi.org/10.2166/wst.2015.023.
[6] S. Lackner, E.M. Gilbert, S.E. Vlaeminck, A. Joss, H. Horn, M.C.M. van Loosdrecht, Full-scale partial nitritation/anammox experiences - An application survey, Water Res. 55 (2014) 292–303, http://dx.doi.org/10.1016/j.watres.2014.02.032.
[7] Y. Ueno, M. Fujii, Three years experience of operating and selling recovered struvite from full-scale plant, Environ. Technol. 22 (2001) 1373–1381, http://dx.doi.org/10.1080/09593332208618196.
[8] W.R. Abma, W. Driessen, R. Haarhuis, M.C.M. Van Loosdrecht, Upgrading of sewage treatment plant by sustainable and cost-effective separate treatment of industrial wastewater, Water Sci. Technol. 61 (2010) 1715–1722, http://dx.doi.org/10.2166/wst.2010.977.
[9] S. Mann, Biomineralization: Principles and Concepts in Bioinorganic Materials Chemistry, Oxford University Press, 2001.
[10] E. Arvin, Observations supporting phosphate removal by biologically mediated chemical precipitation. A review, Water Sci. Technol. 15 (1983) 43–63.
[11] M. Maurer, D. Abramovich, H. Siegrist, W. Gujer, Kinetics of biologically induced phosphorus precipitation in waste-water treatment, Water Res. 33 (1999) 484–493, http://dx.doi.org/10.1016/S0043-1354(98)00221-8.
[12] M.K. De Kreuk, J.J. Heijnen, M.C.M. Van Loosdrecht, Simultaneous COD, nitrogen, and phosphate removal by aerobic granular sludge, Biotechnol. Bioeng. 90 (2005) 761–769, http://dx.doi.org/10.1002/bit.20470.
[13] A. Mañas, B. Biscans, M. Spérandio, Biologically induced phosphorus precipitation in aerobic granular sludge process, Water Res. 45 (2011) 3776–3786, http://dx.doi.org/10.1016/j.watres.2011.04.031.
[14] Y.M. Lin, T. Lotti, P.K. Sharma, M.C.M. van Loosdrecht, Apatite accumulation enhances the mechanical property of anammox granules, Water Res. 47 (2013) 4556–4566, http://dx.doi.org/10.1016/j.watres.2013.04.061.
[15] A. Dapena-Mora, J.R. Vázquez-Padín, J.L. Campos, A. Mosquera-Corral, M.S.M. Jetten, R. Méndez, Monitoring the stability of an Anammox reactor under high salinity conditions, Biochem. Eng. J. 51 (2010) 167–171, http://dx.doi.org/10.1016/j.bej.2010.06.014.
[16] H. Li, Q.Z. Yao, S.H. Yu, Y.R. Huang, X.D. Chen, S.Q. Fu, G.T. Zhou, Bacterially mediated morphogenesis of struvite and its implication for phosphorus recovery, Am. Mineral. 102 (2017) 381–390, http://dx.doi.org/10.2138/am-2017-5687.
[17] A. Sinha, A. Singh, S. Kumar, S.K. Khare, A. Ramanan, Microbial mineralization of struvite: A promising process to overcome phosphate sequestering crisis, Water Res. 54 (2014) 33–43, http://dx.doi.org/10.1016/j.watres.2014.01.039.
[18] A. Soares, M. Veesam, F. Simoes, E. Wood, S.A. Parsons, T. Stephenson, Bio-Struvite: A new route to recover phosphorus from wastewater, Clean - Soil, Air, Water 42 (2014) 994–997, http://dx.doi.org/10.1002/clen.201300287.
[19] European Commission, COM 157 Proposal for a regulation of the European Parliament and of the Council laying down rules on the making available on the market of CE marked fertilising products and amending Regulations (EC) No 1069/2009 and (EC) No 1107/2009, (2016). doi: 10.1017/CBO9781107415324.004.
[20] J. Driver, D. Lijmbach, I. Steen, Why recover phosphorus for recycling, and how?, Environ Technol. 20 (1999) 651–662.

[21] APHA, Standard Methods for the Examination of Water and Wastewater, 19th Ed., American Public Health Association, Washington DC, USA, 2005.
[22] W.J. Schipper, A. Klapwijk, B. Potjer, W.H. Rulkens, B.G. Temmink, F.D. Kiestra, A.C. Lijmbach, Phosphate recycling in the phosphorus industry, Environ. Technol. 22 (2001) 1337–1345, http://dx.doi.org/10.1080/09593330.2001.9619173.
[23] E. Valsami-Jones, Calcium phosphate precipitation, SCOPE Newsl. #41. (2001) 8–15.
[24] W.A. House, The physico-chemical conditions for the precipitation of phosphate with calcium, Environ. Technol. 20 (1999) 727–733, http://dx.doi.org/10.1080/09593332008616867.
[25] J. Mortvedt, Heavy metal contaminants in inorganic and organic fertilizers, Fertil. Res. 43 (1996) 55–61, http://dx.doi.org/10.1007/BF00747683.
[26] G. Nziguheba, E. Smolders, Inputs of trace elements in agricultural soils via phosphate fertilizers in European countries, Sci. Total Environ. 390 (2008) 53–57, http://dx.doi.org/10.1016/j.scitotenv.2007.09.031.
[27] European Commission, Proposal for a Regulation on the making available on the market of CE marked fertilising products and amending regulations (EC) No 1069/2009 and (EC) No 1107/2009 Annexes 1 to 5, (2016). doi:10.1017/CBO9781107415324.004.
[28] J.W. Mullin, Crystallization, 4th ed., Elsevier, Oxford, U.K., 2011.
[29] T. Tervahauta, R.D. van der Weijden, R.L. Flemming, L. Hernández Leal, G. Zeeman, C.J.N. Buisman, Calcium phosphate granulation in anaerobic treatment of black water: A new approach to phosphorus recovery, Water Res. 48 (2014) 632–642, http://dx.doi.org/10.1016/j.watres.2013.10.012.
[30] E. Desmidt, K. Ghyselbrecht, Y. Zhang, L. Pinoy, B. Van der Bruggen, W. Verstraete, K. Rabaey, B. Meesschaert, Global phosphorus scarcity and full-scale p-recovery techniques: a review, Crit. Rev. Environ. Sci. Technol. 45 (2015) 336–384, http://dx.doi.org/10.1080/10643389.2013.866531.
[31] J. Vázquez-Padín, A. Mosquera-Corral, J.L. Campos, R. Méndez, N.P. Revsbech, Microbial community distribution and activity dynamics of granular biomass in a CANON reactor, Water Res. 44 (2010) 4359–4370, http://dx.doi.org/10.1016/j.watres.2010.05.041.
[32] M. Nielsen, A. Bollmann, O. Sliekers, M. Jetten, M. Schmid, M. Strous, I. Schmidt, L.H. Larsen, L.P. Nielsen, N.P. Revsbech, Kinetics, diffusional limitation and microscale distribution of chemistry and organisms in a CANON reactor, FEMS Microbiol. Ecol. 51 (2005) 247–256, http://dx.doi.org/10.1016/j.femsec.2004.09.003.
[33] M. Strous, J.J. Heijnen, J.G. Kuenen, M.S.M. Jetten, The sequencing batch reactor as a powerful tool for the study of slowly growing anaerobic ammonium-oxidizing microorganisms, Appl. Microbiol. Biotechnol. 50 (1998) 589–596, http://dx.doi.org/10.1007/s002530051340.
[34] M.K.H. Winkler, R. Kleerebezem, J.G. Kuenen, J. Yang, M.C.M. van Loosdrecht, Segregation of biomass in cyclic anaerobic/aerobic granular sludge allows the enrichment of anaerobic ammonium oxidizing bacteria at low temperatures, Environ. Sci. Technol. 45 (2011) 7330–7337, http://dx.doi.org/10.1021/es201388t.
[35] Y.Q. Liu, G.H. Lan, P. Zeng, Size-dependent calcium carbonate precipitation induced microbiologically in aerobic granules, Chem. Eng. J. 285 (2016) 341–348, http://dx.doi.org/10.1016/j.cej.2015.10.020.
[36] SCB, Utsläpp till vatten och slamproduktion 2014 - Kommunala reningsverk, massa- och pappersindustri samt viss övrig industri, 2014.